Nuclear spin orientation by electrical spin injection in an $Al_xGa_{1-x}As/GaAs$ spin-polarized light-emitting diode

P. Van Dorpe,* W. Van Roy, J. De Boeck, and G. Borghs
IMEC, Kapeldreef 75, B-3001 Leuven, Belgium
(Received 10 January 2005; revised manuscript received 3 May 2005; published 8 July 2005)

We investigate dynamical nuclear polarization in bulk GaAs by electrical spin injection from a MnSb ferromagnetic top contact using the oblique Hanle effect to examine the circular polarization of the electroluminescence in a spin-polarized light-emitting diode. Reversing the MnSb magnetization or the external field leads to a slow response of the nuclear magnetization, which is reflected in slow changes of the optical circular polarization. Applying an ac-magnetic field at the resonance frequencies of the Ga and As isotopes results in a partial destruction of the nuclear polarization. This also showed that the ^{75}As nuclei are only weakly polarized. We correlate this to the combination of a higher spin relaxation time of the ^{75}As nuclei and the relatively long electron-nucleus-interaction time. We furthermore examined the width of the zero-field dip in the Hanle curve and explain its larger size in terms of an equilibrium between nuclear spin pumping by the electrons and nuclear relaxation.

DOI: 10.1103/PhysRevB.72.035315 PACS number(s): 72.25.Hg, 72.25.Pn, 72.25.Rb, 76.60.Jx

I. INTRODUCTION

It is known that spin-polarized electrons in the conduction band of GaAs create a polarization of the nuclear spins in the GaAs lattice through cooling of the nuclear spin system by the hyperfine interaction. The magnitude of this polarization depends on the localization of the electron wave function and the amount of electrons that are involved. In early experiments, a large nuclear spin polarization due to optical pumping has been detected in compensated samples, where electron localization on donor sites takes place.[1] In recent experiments electrical spin injection from a Fe contact in a GaAs quantum well resulted in a steady state nuclear polarization.[2]

In this paper, we discuss the effects of electrical spin injection from a MnSb contact into an $Al_xGa_{1-x}As/GaAs$-based spin light emitting diode (LED) on the polarization of the nuclei in the GaAs bulk active region. The uniaxial anisotropy and the high coercivity of the MnSb ferromagnetic film allows us to control the sign and the magnitude of the injected spins and the magnetic field independently. We demonstrate real-time transient effects in the electronic spin polarization that can be associated with a slow change of the nuclear polarization when the sign of the injected spins is reversed. Furthermore we show that a reversal of the magnetic field results in an adiabatic reversal of the nuclear spin polarization. Using these transient effects, we were able to measure the nuclear spin relaxation time due to both the hyperfine interaction and the relaxation time in the absence of electrons. Finally, to further investigate the behavior of the nuclei, we bring the nuclear spins into resonance using an oscillating magnetic field and look at the effect on the electron spins. From the nuclear magnetic resonance measurements and the field and bias dependence of the nuclear relaxation times we explain the magnitude and the bias dependence of the low-field nuclear depolarization.

II. EXPERIMENTS

We have studied spin injection from epitaxial MnSb layers into GaAs through a Schottky barrier. Since the surface Fermi level is pinned around the middle of the (Al,Ga)As band gap, the semiconductor region in the vicinity of the interface is heavily doped to obtain a narrow Schottky barrier that allows tunneling.[3] Through the Schottky barriers, larger electron injection currents can be achieved than through oxide barriers, which is important for nuclear polarization.[4,5] The structure is described in Table I. Figure 1 shows the simulated band structure of the spin LED under bias.[6] The band structure and the doping profile of the LED were designed such that under bias the spin-polarized electrons tunnel through the highly *n*-type doped (Al,Ga)As interfacial region and then travel through a lightly *n*-type doped (Al,Ga)As region to a GaAs active region. In the GaAs region the electrons thermalize and recombine with holes supplied from the *p*-type substrate. The entire layer structure is grown by molecular beam epitaxy (MBE). After the growth the wafers are processed into devices with lateral dimensions of 40×40 μm by means of optical lithography and wet etching techniques.

TABLE I. The spin-LED structure.

Thickness	Material	Doping
5 nm	GaAs cap	—
10 nm	MnSb	—
8 nm	$Al_{0.1}Ga_{0.9}As$	$n=1.5\times10^{19}$ cm^{-3}
5 nm	$Al_{0.1}Ga_{0.9}As$	$n=7.5\times10^{18}$ cm^{-3}
10 nm	$Al_{0.1}Ga_{0.9}As$	$n=3\times10^{18}$ cm^{-3}
20 nm	$Al_{0.1}Ga_{0.9}As$	$n=3\times10^{17}$ cm^{-3}
20 nm	$Al_{0.1}Ga_{0.9}As$	$n=5\times10^{16}$ cm^{-3}
100 nm	GaAs	*i*
20 nm	$Al_{0.3}Ga_{0.7}As$	*i*
180 nm	$Al_{0.3}Ga_{0.7}As$	$p=10^{18}$ cm^{-3}
1 μm	GaAs	$p=10^{18}$ cm^{-3}
Substrate	GaAs	$p=10^{18}$ cm^{-3}

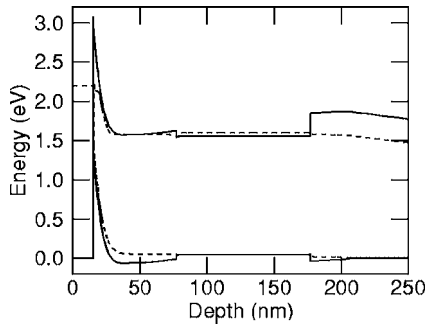

FIG. 1. The simulated band structure of the spin LED under bias (2.2 V) at 80 K. The dashed lines indicate the quasi-Fermi levels for electrons and holes.

MnSb is a ferromagnetic material that is particularly suited to study the effects of the magnetization on the nuclear polarization in GaAs. It has the hexagonal NiAs crystal structure resulting in a strong magnetocrystalline anisotropy with the *c* axis as hard direction and the basal plane as easy plane. For a substrate temperature of 250 °C MnSb grows on GaAs(001) in the $(1\bar{1}01)$ orientation, with the projection of the *c* axis aligned along the GaAs[110] direction.[7] The shape anisotropy requires the easy magnetization direction(s) to be in the plane of the film. The magnetocrystalline anisotropy of MnSb reduces the symmetry within this plane and results in an easy in-plane direction along $[1\bar{1}0]$, and a hard direction orthogonal to this, along [110]. This is clearly shown by the in-plane magnetization loops measured with an alternating gradient field magnetometer (AGFM) parallel to the $[1\bar{1}0]$ and the [110] directions (Fig. 2).[4] The $[1\bar{1}0]$ easy direction exhibits square loops with a relatively large coercive field,

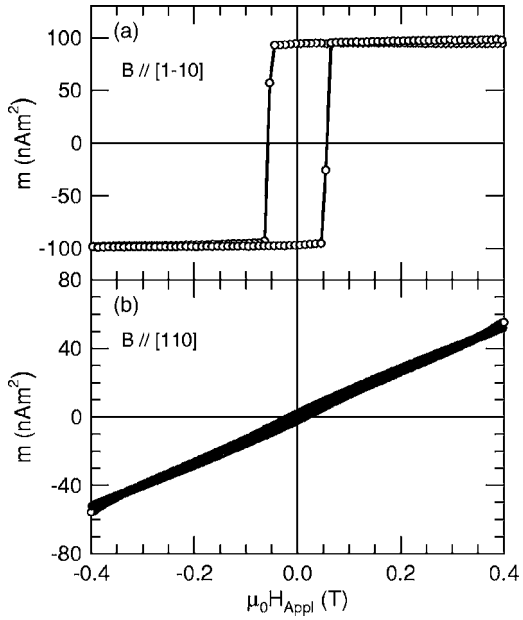

FIG. 2. (a) The magnetization of the MnSb film as a function of the magnetic field in the $[1\bar{1}0]$ direction. (b) The magnetization of the MnSb film as a function of the magnetic field in the [110] direction.

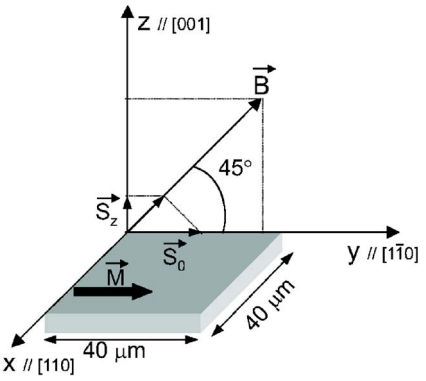

FIG. 3. Schematic picture of the measurement geometry. The LED has been patterned in devices of 40×40 μm (grey area). The magnetic field is applied in an angle of 45° with respect to the plane, with its in-plane component along the easy axis of the MnSb film. The light is collected along the sample normal.

which allows us to visualize the effects of the magnetization on the Hanle curve. An out-of-plane AGFM measurement (not shown) showed a hard-axis behavior with the saturation magnetization of the film equal to $\mu_0 M_S = 0.8$ T.

A. Oblique Hanle effect technique

To measure the steady-state spin polarization in the GaAs active region, we analyze the degree of circular polarization of the emitted light of the (surface-emitting) spin LED using the oblique Hanle effect technique.[8,9] The measurement geometry is sketched in Fig. 3. The circular polarization of the emitted light is only sensitive to the perpendicular spin component. By applying a small oblique magnetic field, with its in-plane component along the $[1\bar{1}0]$ easy direction of MnSb, spin precession forces the average spin to come out of plane and to eventually align with the field.

In contrast to the normal Hanle effect, the magnetic field has a component parallel to the injected electron spins, which allows nuclear polarization to occur and to be observed. The injected spin-polarized electrons transfer their angular momentum to the nuclear spins through the hyperfine interaction—they pump the nuclear spin system. The polarized nuclei generate an effective magnetic field acting on the electron spins that is superimposed on the external field. This effective field can be significantly larger than the applied field. At low fields, comparable to the local dipole fields, the nuclear magnetization collapses and there occurs a sharp dip in the circular polarization.

The dependence of the average spin in the semiconductor on the external magnetic field can be calculated from the Bloch equations[1]

$$\frac{d\mathbf{S}}{dt} = \mathbf{\Omega} \times \mathbf{S} - \frac{\mathbf{S}}{\tau_S} - \frac{\mathbf{S} - \mathbf{S}_0}{\tau}, \tag{1}$$

with $\mathbf{S}$ the average spin, $\mathbf{S_0}$ the injected average spin, τ the electron-hole recombination time, and τ_S the spin-relaxation time. The circular polarization is proportional to the perpendicular spin component S_Z and can in the oblique Hanle effect geometry be calculated to be[9]

$$P(\Omega) = \frac{\Pi_{\text{inj}} \times \cos(\theta)}{2} \frac{T_S}{\tau} \frac{(\Omega \times T_S)^2 \cos(\phi)\sin(\phi)}{1 + (\Omega \times T_S)^2} + \frac{\Pi_{\text{inj}} \times \sin(\theta)}{2} \frac{T_S}{\tau} \frac{1 + (\Omega \times T_S)^2 \cos^2(\phi)}{1 + (\Omega \times T_S)^2}, \quad (2)$$

with Π_{inj} the degree of injected spin polarization, $T_S^{-1} = \tau^{-1} + \tau_S^{-1}$. θ is the angle between the sample plane and the magnetization and ϕ the angle between the applied magnetic field and the sample plane, which equals 45° in these experiments, as indicated in Fig. 3.

$$\mathbf{\Omega} = \frac{g^* \mu_B}{\hbar}(\mathbf{B} + \mathbf{B}_n), \quad (3)$$

with g^* the effective g factor, μ_B the Bohr magneton and $\hbar$ Planck's constant, and $\mathbf{B}$ the external field.

The total field that the electron spins experience is the superposition of the external field $\mathbf{B}$ and the nuclear field $\mathbf{B_N}$, which can be described as follows[1]

$$\mathbf{B_n} = b_n \cdot \mathbf{B} \frac{\mathbf{s} \cdot \mathbf{B}}{B^2 + B_{\text{loc}}^2}, \quad (4)$$

with $\mathbf{s}$ the unit vector in the direction of the average spin, $\mathbf{B_n}$ the effective nuclear field acting on the electron spins, B_{loc} the local random field that the nuclei experience, and b_n is the (scalar) high-field value of $\mathbf{B_n}$ (when $\mathbf{s} \| \mathbf{B}$ and $B \gg B_{\text{loc}}$)

$$b_n = f \times b_{ni} \frac{I(I+1)}{S(S+1)} \langle S \rangle, \quad (5)$$

with $S=1/2$, $I=3/2$. $f=T_1/(T_1+T_{1e})$ is the leakage factor where T_{1e} and T_1 are, respectively, the nuclear relaxation time due to the hyperfine interaction with the spin-polarized electrons and the nuclear relaxation time due to other mechanisms. $\langle S \rangle$ is the average electron spin. For one isotope b_{ni} can be expressed as follows:[1]

$$b_{ni} = \frac{16\pi}{3g^* v_0} \mu_I \eta \xi \quad (6)$$

with μ_I the nuclear magnetic moment, v_0 the volume of one unit cell, η the electron density in one unit cell, and ξ the number of nuclei of the considered isotope in the unit cell. The measured nuclear field is always the sum of the respective nuclear fields of the different isotopes, so we use a single b_{ni}.

B. Transient effects

1. Initial observations

Figure 4 shows the measured degree of circular polarization of the electroluminescence of the sample as a function of the oblique magnetic field. The circles are measurement data from a "slow" scan: After adjusting the value of the magnetic field, there is a pause of one minute before measuring the degree of circular polarization, while the current is continuously flowing through the device. The triangles represent a "fast" scan: In this case there is a pause of only one second after a change of the field. The slow measurement

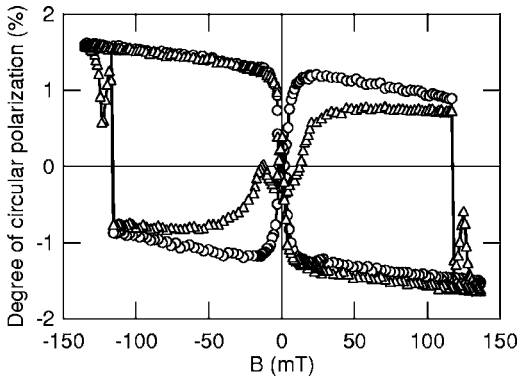

FIG. 4. The circular polarization of the electroluminescence as a function of the external field at 5 K and 750 A/cm^2. (△): fast measurement: one datapoint per second, (○): slow measurement: a pause of 60 s after changing the external field.

shows a Lorentzian shaped curve, which is characteristic for an oblique Hanle measurement. The saturation field of the circular polarization is only about ~10 mT, which, without the assumption of a nuclear field would imply a very long electron spin lifetime (~10 ns). An independent optical pumping experiment (not shown),[9] however, showed a much smaller $T_S \sim 200$ ps. The reason for this discrepancy is the presence of a strong nuclear field that results in an external field dependence mimicking the oblique Hanle effect signature: It accelerates spin precession and saturates the optical polarization already in small fields, but vanishes around zero field. This is furthermore corroborated by the findings of the fast measurement. This measurement looks quite different, there are transient effects present at the reversal of the magnetic field and at the reversal of the MnSb magnetization. It seems that at these points, the effective magnetic field caused by nuclear spins changes more slowly than the applied magnetic field. To clarify these effects, we have performed three types of measurements. (1) The sign of the injected electron spins is changed, keeping the external magnetic field constant. (2) The sign of the injected electron spins is kept constant, but the external magnetic field is reversed. (3) Both the injected electron spins and the external magnetic field are reversed. During the changes we switch off the device current, such that during the reversing of the magnetic field, or the reversing of the magnetization, the electron spins do not influence the nuclear spins. Immediately after the manipulation, the current is switched back on and the circular polarization of the light is monitored as a function of the laboratory time.

We will now discuss the three experiments. In a first measurement, shown in Fig. 5, the original value of the magnetic field is (−)100 mT. Next, after switching off the current, the MnSb magnetization is reversed by sweeping the field to (−)130 mT and returning to (−)100 mT. After this, the current is switched back on and the circular polarization of the light is monitored. The data show that the circular polarization decreases, reaches a minimum, and increases again up to its original value. This measurement indicates that the nuclear spins, which have not changed during the dark period, are slowly reversed by the electron spins. This causes

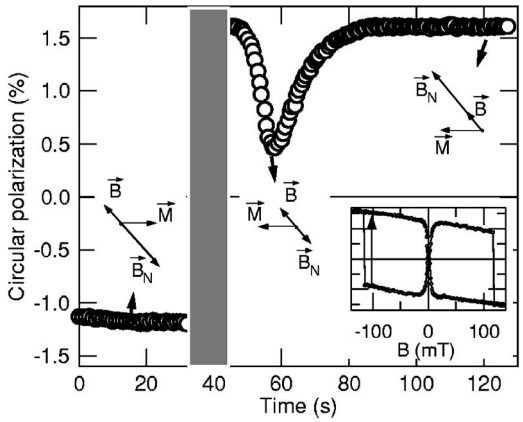

FIG. 5. The degree of circular polarization of the electroluminescence versus time after reversing the magnetization of the MnSb in a negative external field at 5 K and 750 A/cm^2. During the gray period the current through the device is switched off and the magnetization is reversed. A magnetization reversal in a positive external magnetic field gives the same result. The bottom right inset shows the full Hanle curve, which schematically shows that we reverse the MnSb magnetization. The vector diagrams show the relative orientation of the magnetization **M**, the applied field **B**, and the nuclear field $\mathbf{B_N}$ during the time sweep.

the nuclear field and thus the total field acting back on the electron spins to decrease, reverse sign, and increase again, resulting in a dip in the circular polarization.

In Fig. 6 a similar experiment is shown, but instead of the electron spins, the magnetic field is reversed in the dark period. The field is swept from ± 63 to ∓ 63 mT. The field sweep ($\sim$4 mT/s) is slow in comparison to the transverse nuclear spin lifetime T_2 ($\sim$100 μs), which means that at all times, the nuclear spin ensemble is in internal equilibrium. A characteristic dip similar to the previous experiment appears

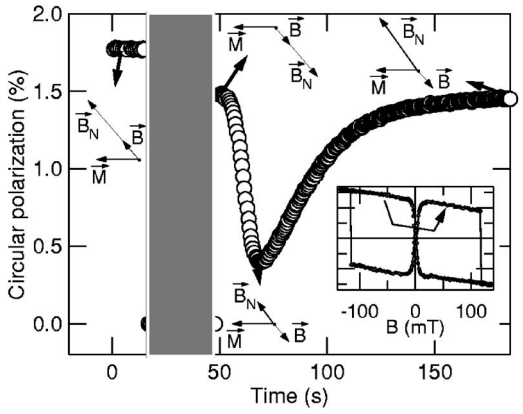

FIG. 6. The degree of circular polarization versus time after reversing the external field from -63 to $+63$ mT at 5 K and 750 A/cm^2. During the gray period the current through the device is switched off and the field is reversed. Reversing the field from $+63$ to -60 mT gives the same result. The bottom right inset shows the full Hanle curve, which schematically shows that we reverse the sign of the external magnetic field. The vector diagrams show the relative orientation of the magnetization **M**, the applied field **B**, and the nuclear field $\mathbf{B_N}$ during the time sweep.

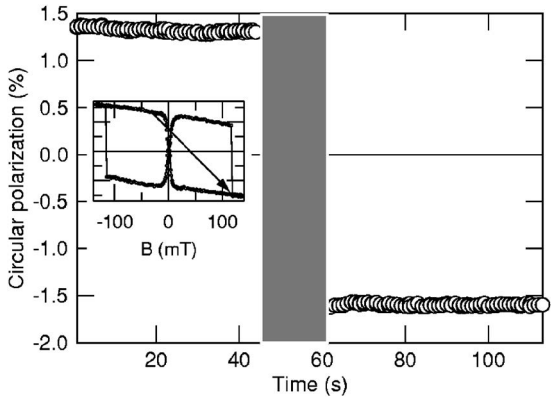

FIG. 7. The degree of circular polarization of the electroluminescence versus time after reversing both the external field and the MnSb magnetization at 5 K and 750 A/cm^2. The inset shows the full Hanle curve, which schematically shows that we reverse the sign of both the external magnetic field and the MnSb magnetization.

in the circular polarization. The appearance of this dip suggests that during the reversal of the magnetic field, the nuclear spins have changed sign. After the electron spin injection is switched on again, the electron spins can slowly force the nuclear spin back to their original position, i.e., aligned with the electrons spins. To check this hypothesis, we have performed a similar measurement, but in this case reversing both the electron spins and the magnetic field.

Figure 7 shows that when the field is swept from ± 30 to ∓ 130 mT, no transient effects occur in the degree of circular polarization. Because both the electron spins and the nuclear spins have reversed in the dark period, no transient behavior is expected.

2. Measurements of the nuclear relaxation time and the nuclear field

The slow reversal of the nuclear field due to the hyperfine interaction allows us to measure the nuclear spin relaxation time due to the hyperfine interaction. The rate equation for the evolution of the nuclear spin system is given by[10]

$$\frac{\langle I_z\rangle}{dt} = -\frac{1}{T_{1e}}\left[\langle I_z\rangle - \langle S\rangle \frac{I(I+1)}{S(S+1)}\right] - \frac{1}{T_1}\langle I_z\rangle, \tag{7}$$

with $\langle I_z\rangle$ the average nuclear spin parallel to the magnetic field and $\langle S\rangle$ the average electron spin. This leads to a steady-state average nuclear spin given by

$$\langle I_z\rangle = \frac{I(I+1)}{S(S+1)}\frac{T_1}{T_{1e}+T_1}\langle S\rangle. \tag{8}$$

Giving that the GaAs active layer is not intentionally doped and that the electroluminescence spectrum shows band-to-band emission, the dominant nuclear relaxation mechanism is due to free (conduction) electrons. This implies that the relaxation time T_{1e} is given by[11]

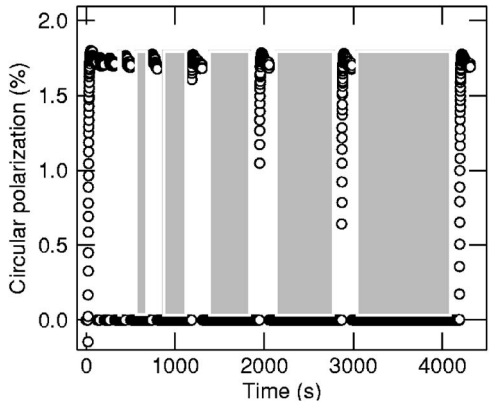

FIG. 8. Nuclear depolarization curve at 5 K and 18 mT. The device current is switched off during increasing time intervals (grey areas) and switched on again.

$$T_{1e}^{-1} = \frac{32}{9}\gamma_e^2 \times \gamma_n^2 \times n \times \eta^2 (2\pi m^3 kT)^{1/2}, \tag{9}$$

with γ_e and γ_n the electronic and the nuclear gyromagnetic ratios, respectively. n is the carrier concentration and η the electronic density at the nucleus.

Using GaAs parameters,[1] at a temperature of 5 K, and a carrier concentration of 4×10^{17} cm^{-3}, we get an estimated $T_{1e}=27$ s.

When the injected electron spins have changed sign due to the reversing of the MnSb magnetization or when the nuclear polarization has been adiabatically reversed, the nuclear polarization (corresponding originally to a nuclear field b_{n0}) will, according to Eq. (7), exponentially evolve toward its new equilibrium value (corresponding to a nuclear field b_{n1}), with a time constant T_{1e}. To fit the curves in Figs. 5 and 6, we use Eq. (2), with a nuclear field that varies exponentially with time using a time constant $\tau = T_1 \times T_{1e}/(T_1+T_{1e})$,

$$b_n = b_{n1} - (b_{n1} - b_{n0})\exp[-(t-t_0)/\tau]. \tag{10}$$

We have used the nuclear field at the start of the sweep b_{n0}, at the end of the sweep b_{n1} and the time constant τ as fit parameters. The injected spin polarization is determined from the full Hanle curve and the spin lifetime T_S in the GaAs active region is determined to be 200 ps by an independent optical pumping experiment (not shown).

a. Nuclear spin-lattice relaxation time T_1. To investigate the decay time of the nuclear polarization due to direct coupling to the lattice, without the presence of electrons, we monitored the circular polarization of the light, while we switched off the current during increasing time intervals. By analyzing the initial circular polarization after switching the current back on (Fig. 8), the nuclear spin-lattice relaxation time T_1 can be deduced. During the time that the current is switched off, T_{1e} can be considered as infinite and τ equals T_1. From a measurement shown in Fig. 8 at 4.6 K and 17.8 mT, T_1 can be deduced to be near 7.5 min. This time strongly depends on the value of the external magnetic field, as shown in Fig. 9.

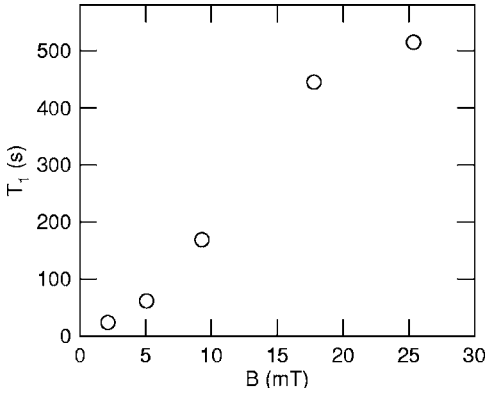

FIG. 9. The nuclear spin-lattice relaxation time T_1 as a function of the external magnetic field at 5 K.

b. The nuclear spin relaxation time due to the hyperfine interaction T_{1e}. To investigate the hyperfine interaction time T_{1e}, we analyze the transient effects that occur in Figs. 5 and 6. In order to obtain a measure of T_{1e}, we use a measurement at relatively high field, where $T_1 \gg T_{1e}$, such that τ equals T_{1e}. It appears that there is a nonhomogeneous distribution of the time constant over the sample. If the switching of the nuclear polarization would be describable by just one time constant and a homogeneous nuclear field, at one point during the nuclear spin reversal process the nuclear field would exactly cancel the external field and the circular polarization should go through zero. We have not observed such a phenomenon, which indicates that the nuclear polarization is not homogeneous. We have used a linear distribution for the time constant to take this into account. The fit of the transient curve in Fig. 10 gives a time constant that is distributed between 24 and 60 s. The weight is maximal at 24 s and decreases linearly toward zero at 60 s. The fit value of the nuclear field is about 1 T. The inhomogeneous distribution of the nuclear polarization may be explained by a nonhomogeneous distribution of the carrier concentration in the active GaAs region. In Fig. 11 the simulated electron concentration is shown in the active region as a function of the depth. The simulations show that the electron concentration is not uniform across the active region but has a maximum near the top AlGaAs barrier.

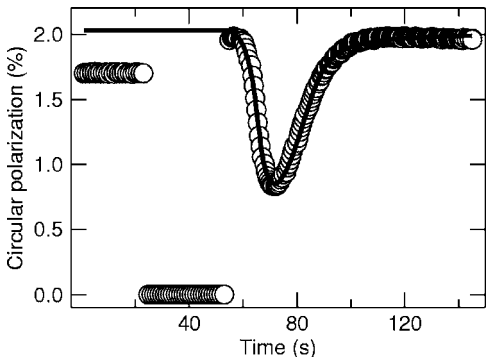

FIG. 10. Transient behavior of the circular polarization after reversing the external magnetic field at 5 K and 750 A/cm^2 (○), together with the fit (solid line) based on Eq. (10). Fit parameters: $T_{1e}=24$ s, $b_N \sim 1$ T.

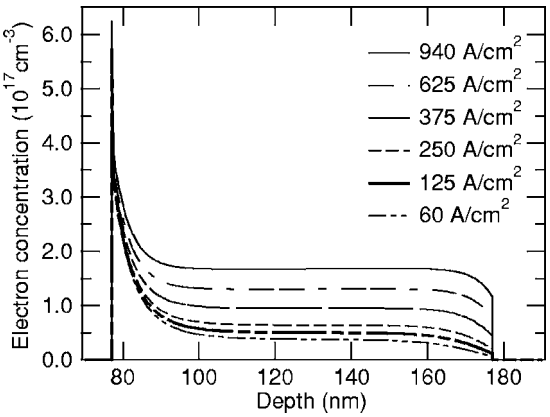

FIG. 11. The simulated electron concentration in the GaAs active region as a function of the depth for different values of the current density. The concentration is the highest near the top AlGaAs barrier.

c. Temperature and bias dependence of the time constant T_{1e}. The characteristic time constant of the hyperfine interaction T_{1e} decreases with temperature, as shown in Fig. 12 and indicated by Eq. (9). The behavior as expected from Eq. (9) is shown by the solid line. There are a few reasons why the actual behavior deviates from the expected. There is an error on the temperature readout. Since the current density through the device is quite high, the actual temperature in the device is probably several degrees above the measured value. Furthermore, the expected behavior is based on a carrier concentration of 4×10^{17} cm^{-3}. As is shown in Fig. 11, the electron concentration within the active region is very inhomogeneous. This causes an inhomogeneous nuclear polarization and time constant within the active region. It is difficult to estimate how the effective electron concentration changes as a function of the temperature.

According to Eq. (9) the time constant $T_{1e}\sim n^{-1}$. Higher injection currents hence lead to smaller T_{1e}. In Fig. 13, T_{1e} is shown as a function of a the applied current. Indeed T_{1e} decreases with increasing bias, consistent with Eq. (9). The plotted T_{1e} corresponds to the time constant with the maximal weight in the fit. At lower bias the distribution of the

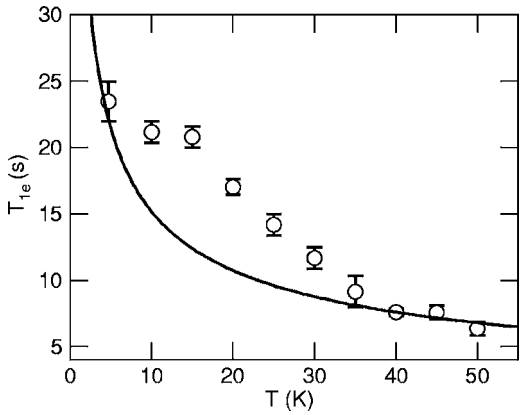

FIG. 12. T_{1e} as a function of the temperature (○) at 750 A/cm^2, together with the theoretical expected behavior (solid line) based on Eq. (9).

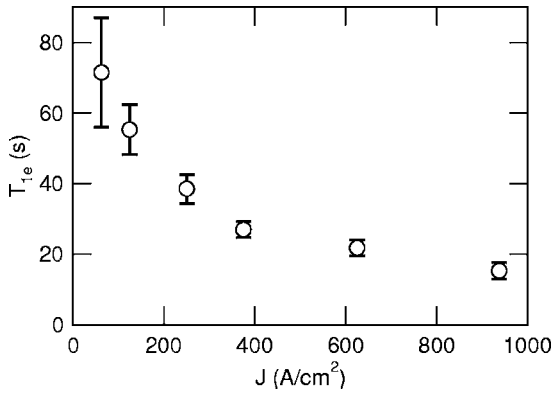

FIG. 13. T_{1e} as a function of the bias current density at 5 K.

time constants shifts toward a larger time constant, as indicated in Fig. 13, but the distribution still has a tail at lower time constants (to about 10 s). This could be explained by the non-homogeneous distribution of the electron concentration in the active GaAs region. Although the average concentration in the active region changes strongly with applied bias, the peak concentration near the top AlGaAs barrier is less sensitive to the bias, as is shown in Fig. 11.

d. Bias dependence of the nuclear field b_n. The fitting procedure of the transient effects of the electroluminescence allows us not only to obtain a value of the time constants involved, but also the absolute value of the nuclear field. In Fig. 14 the dependence of this fitted nuclear field is shown as a function of the bias. At low values of the nuclear field we can verify this procedure by direct visualization of the nuclear field. At negative values of the external magnetic field the nuclear field is aligned antiparallel to the external field. The effective field for the electrons is the superposition of both the external magnetic as the nuclear field. When the external field equals the nuclear field, there is no precession and hence there should be no circular polarization. Due to the limited coercivity of the MnSb film, this field cannot be reached. However, due to the slow response of the nuclear spin system upon external changes, we can bypass this problem. When we use the procedure described in Sec. II B and Fig. 5 to visualize the transient effects after a reversal of the magnetization, and sweep the magnetic field to different val-

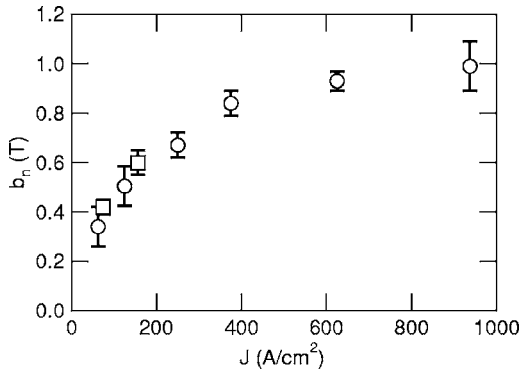

FIG. 14. b_n as a function of the bias current density at 5 K obtained through the fitting procedure (○) and through the field dependence of the transient effects (□).

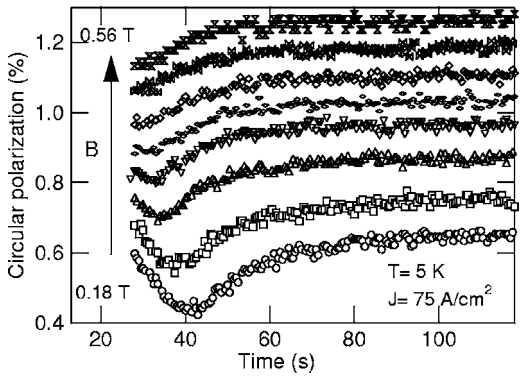

FIG. 15. Transient effects in the circular polarization upon a reversal of the magnetization for different values of the external field at a current density of 75 A/cm^2 and a temperature of 5 K. The applied field goes from 0.18 to 0.56 T. The curves are offset for clarity.

ues before switching on the device current, we can monitor the initial behavior of the circular polarization as a function of the time for different values of the magnetic field. If the external field is smaller than the nuclear field when the device current is switched back on, the current-induced reversal of the nuclear field causes a dip in the circular polarization, since the effective field for the electrons first decreases until $B=B_N$, before increasing again. If the external field exceeds the nuclear field, only an increase of the polarization is expected, since the effective field for the electrons only increases in this case. This is shown in Figs. 15 and 16 for different values of the current density. In Fig. 15 there is a transition from a clear dip in the circular polarization to just a slight increase of the circular polarization, while in the case of Fig. 16 this transition is just above the highest applied field. When we then put these values in Fig. 14, they confirm the values obtained by the fitting procedure.

The bias dependence of the nuclear field can be understood based on Eq. (8). The average nuclear spin is proportional to both the average electron spin $\langle S \rangle$ and the factor $T_1/(T_1+T_{1e})$. Since the measured nuclear field has been determined at a relatively high external field, where T_1 exceeds

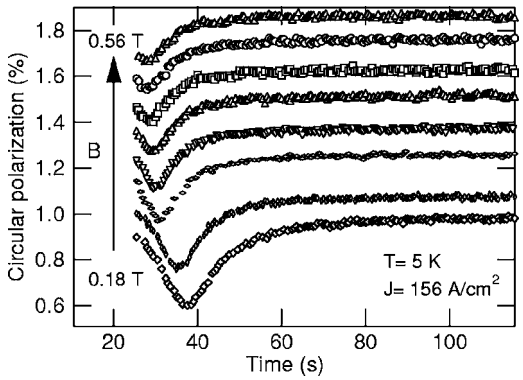

FIG. 16. Transient effects in the circular polarization upon a reversal of the magnetization for different values of the external field at a current density of 156 A/cm^2 and a temperature of 5 K. The applied field goes from 0.18 to 0.56 T. The curves are offset for clarity.

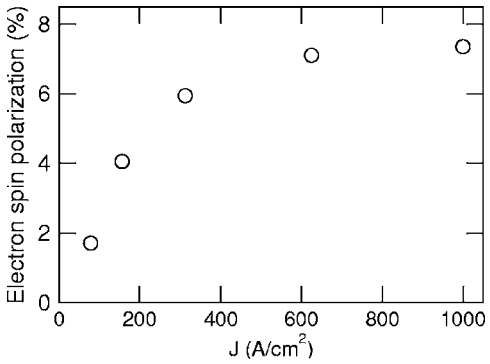

FIG. 17. The steady-state electron spin polarization as a function of the applied current density at 5 K.

500 s, the average nuclear spin is determined by the average electron spin. This is confirmed by a measurement of the bias dependence of the steady-state electron spin polarization in the GaAs active region, as shown in Fig. 17. The steady-state electron spin polarization has been obtained by fitting the full Hanle curves using Eq. (2). The increase of the nuclear field is clearly accompanied by an increase of the steady-state electron spin polarization.

C. Nuclear magnetic resonance

Unambiguous proof of the presence of a nonequilibrium nuclear polarization can be given by investigating the effect of an oscillating magnetic field that brings the nuclei into resonance, nuclear magnetic resonance (NMR).[12] We inserted a coil in the cryostat to generate an ac field which is perpendicular to the direction of the injected spins and to the applied dc field. The ac signal is generated by a signal generator and amplified by a broad-band amplifier.

In order to completely destroy the nuclear polarization the frequency was swept continuously through the resonance frequencies of the different isotopes (^{69}Ga, ^{71}Ga, and ^{75}As) at 5 K. Figure 18 shows the oblique Hanle measurement without applied ac field (○) and while sweeping the frequency between 40 and 700 KHz once a second (△). At low dc fields, when the resonance frequencies were within the scan-

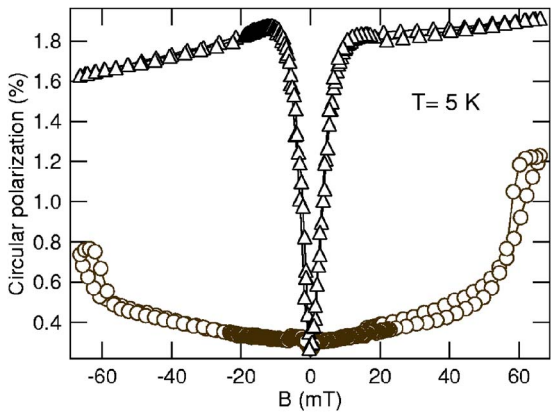

FIG. 18. The Hanle curve without the application of an ac field (△) and while sweeping once per second from 40 to 700 KHz (○).

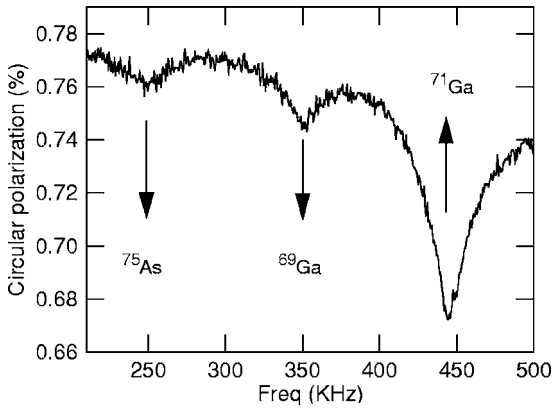

FIG. 19. The circular polarization of the electroluminescence as a function of the frequency of the ac field at 80 K and 35 mT. At the resonance frequencies of the GaAs isotopes a dip in the circular polarization is clearly visible.

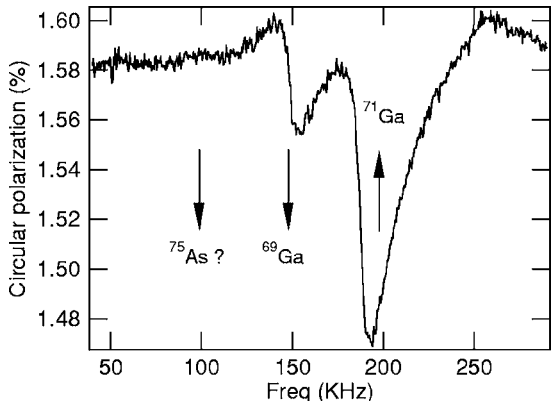

FIG. 21. The circular polarization of the electroluminescence as a function of the frequency of the ac field at 5 K and 15 mT while sweeping from high to low frequency. The resonance signatures of ^{71}Ga and ^{69}Ga can be distinguished.

ning range, the measured circular polarization was completely quenched, indicating a much smaller effective field acting on the electron spins.

Keeping the external field constant and sweeping the frequency slowly through the resonance frequencies allows us to visualize the different isotopes. Figure 19 shows the circular polarization as a function of the frequency of the ac field at 80 K and 35 mT. The As and Ga isotopes can be clearly distinguished and appear at the expected frequency. This is further confirmed when the resonance frequencies are plotted as a function of the applied field in Fig. 20. The resonance frequencies show a linear behavior with magnetic field: 1270 Hz/Oe for ^{71}Ga, 1006 Hz/Oe for ^{69}Ga, and 708 Hz/Oe for ^{75}As, in good agreement with the gyromagnetic ratios: $\gamma(^{71}\text{Ga})=1298$ Hz/Oe, $\gamma(^{69}\text{Ga})=1022$ Hz/Oe, and $\gamma(^{75}\text{As})=729$ Hz/Oe.[1]

At 5 K, the situation changes, the ^{71}Ga nuclei dominate the nuclear field and the ^{75}As resonance cannot even be observed. Figure 21 shows the measured circular polarization at 5 K and at an external field of 15 mT. The frequency was swept from low to high frequency in this measurement. Only the Ga isotopes are clearly visible on this scan. The ^{71}Ga signal is the largest one, while the ^{69}Ga is substantially smaller. The ^{75}As signal is very weak and can be hardly distinguished. This has been consistently observed for different scan speeds, scan directions, and values of the external field. The absence of the ^{75}As signal means that the induced electron spin precession due to the sum of the ^{71}Ga and the ^{69}Ga field is fast enough to saturate the circular polarization. Small changes to the total field because of a change of the ^{75}As field hence have little influence on the degree of circular polarization. This indicates that mainly the ^{71}Ga nuclei and to a smaller extent the ^{69}Ga nuclei are responsible for the nuclear field.

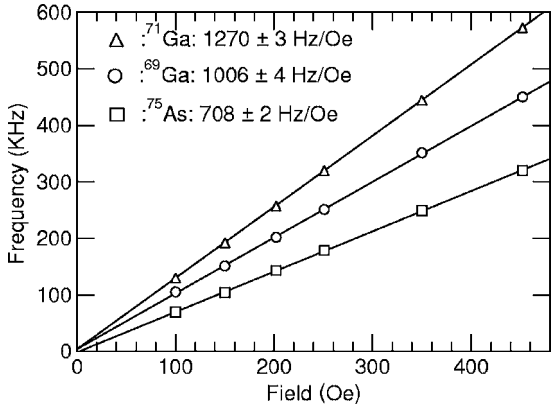

FIG. 20. The measured resonance frequencies of the three isotopes in GaAs as a function of the applied field at 80 K.

III. DISCUSSION

A. Field induced nuclear reversal

The nuclear field reversal during the magnetic field reversal (Figs. 6 and 7 appears to be faster than the time resolution of the measurement and indicates an adiabatic process. The field is swept sufficiently slow such that the nuclear spins can at all times follow the field. Take for example a nucleus that is initially aligned (antialigned) with the field. When the applied magnetic field is lowered, the total field seen by the nucleus is the vector sum of **B** and a local field $\mathbf{B}_{\text{loc}}$. This local field consists of the random dipolar fields induced by the neighboring nuclei *and* the stray field of the MnSb ferromagnetic layer. A magnetostatic simulation shows that this stray field is of the order of 0.2 mT, which is of the same order as the dipolar field. Since we switch off the electron injection during the zero-field traversal, the nuclei do not feel the electronic field. The magnetic field **B** is changed slowly enough compared to the Larmor precession cycle such that the nuclei will remain aligned (antialigned) with the total field. At zero external field, the nucleus will be pointing parallel to $\mathbf{B}_{\text{loc}}$. The average nuclear spin of the sample at that point is zero, since the local fields point in random directions in different parts of the sample, but the degree of alignment of the individual spins with their local field is preserved.[13] If we now turn the magnetic field back on, but in the reversed direction, the nucleus will continue to be aligned (anti-

aligned) with the total field, which causes a reversal of the nuclear spin polarization.

B. Dominance of ^{71}Ga and the low-field nuclear depolarization

At first point it is difficult to understand why the nuclear field is dominated by the ^{71}Ga nuclei. Previous experiments and theoretical calculations showed that the ^{71}Ga nuclei even exert the smallest effective field on the electrons [$b(^{75}\mathrm{As}) = -18.4$ kG, $b(^{69}\mathrm{Ga}) = -9.1$ kG and $b(^{71}\mathrm{Ga}) = -7.8$ kG].[14] This leads to the conclusion that the ^{75}As nuclei are only weakly polarized. A possible explanation lies in the different nuclear relaxation times of the different isotopes. It is known[15] that the most important nuclear relaxation mechanism in GaAs is the quadrupolar relaxation mechanism. The quadrupole moment of As is higher than that of Ga, which causes a smaller nuclear spin lifetime [$T_1(^{71}\mathrm{Ga}) = 6.6 \times T_1(^{75}\mathrm{As})$ and $T_1(^{71}\mathrm{Ga}) = 2.3 \times T_1(^{69}\mathrm{Ga})$]. Since the steady-state nuclear polarization is an equilibrium between pumping and relaxation, the nuclear polarization of the As spins can be significantly smaller when the pumping time is similar to the relaxation time.

More evidence for this is given by the field dependence of the nuclear spin relaxation time at 5 K, which is shown in Fig. 9. The dark nuclear relaxation time strongly decreases with decreasing external field. At high field the nuclei are decoupled and the observed spin relaxation time is mainly given by the ^{71}Ga-spin relaxation time, while at lower fields the interaction between the Ga and the As spins increases such that there is an out diffusion of nuclear spin polarization from the Ga spin bath to the ^{75}As spin bath. The spin relaxation time will then be dominated by the (short) ^{75}As-relaxation time. This can also explain why in previous reports[1,14] the ^{75}As resonance was much stronger. In their case the nuclear polarization was mainly created by electrons that were localized on donor sites. The characteristic hyperfine interaction time for localized electrons is a lot smaller than for conduction electrons ($\sim$0.1 s). Hence, the shorter pumping time (i.e., an increased pumping efficiency) allowed a larger ^{75}As-steady-state polarization.

The resonance signal of ^{75}As is nevertheless visible at 80 K. This could be explained by the overall smaller nuclear field. The nuclear field is not strong enough to completely saturate the Hanle curve such that small changes to the total nuclear field are more easily visible in a frequency scan.

C. Zero-field dip

The half width of the zero-field dip in the Hanle curve in Fig. 4 should correspond to the random local field that the nuclei experience [B_{loc} from Eq. (4)]. Its value, measured in steady-state conditions, is about 7 mT at 4.5 K and 750 A/cm^2. This value is over ten times higher than the optical orientation value of the local dipole field, which is more in the order of 0.2 mT.[1] Other reports also indicate that in different structures and different measurement geometries the local fields seem higher than measured with photoluminescence (PL) in bulk GaAs.[2,16] A solution is offered by the field dependence of the nuclear relaxation time as shown in Fig. 9. At low fields, the nuclear relaxation time becomes comparable to the pumping time induced by the hyperfine interaction with the electron spins. The leakage factor $f = T_1/(T_1 + T_{1e})$ hence decreases strongly with decreasing field and causes a strong decrease of the steady-state nuclear spin polarization with decreasing field

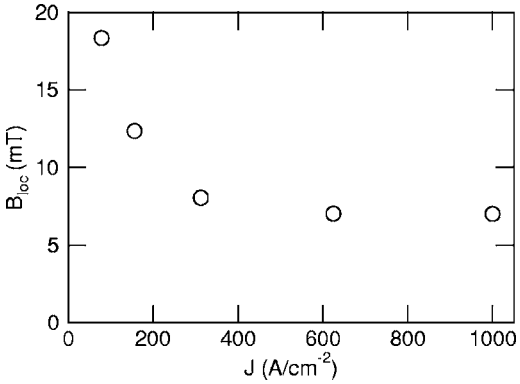

FIG. 22. The apparent local field B_{loc} as a function of the current density at 5 K.

$$B_{n,\text{low field}} = \frac{T_1}{T_{1e} + T_1} B_{n,\text{high field}} \tag{11}$$

under the assumption that $f \approx 1$ at high field.

To test this hypothesis we looked first at the bias dependence of the half width of the zero-field dip. In Fig. 22 the apparent local field B_{loc} is shown as a function of the current density. It is clear that the apparent B_{loc} decreases strongly with increasing electron pumping. B_{loc} has been obtained by fitting the full Hanle curves using Eq. (2), combined with Eq. (4). A similar behavior has been observed before at 80 K.[4] When the bias increases, the electron concentration increases and according to Eq. (9), T_{1e} drops. The drop in T_{1e} hence narrows the dip in the Hanle curve.

In an effort to reconstruct the Hanle curve without the presence of this low-field nuclear relaxation, we measure the circular polarization as a function of time and start with the field high enough such that $T_1 \gg T_{1e}$. We subsequently quickly move the field to a low-field value and monitor the decay of the circular polarization as function of time. The value of the circular polarization immediately after the field change corresponds to the value "without nuclear relaxation." In Fig. 23 such an experiment is shown, where the field was -15 mT originally and has then been swept rapidly to -2.6 mT. It is clear that the circular polarization slowly decays to its steady-state value. This procedure can be performed for many field points around zero field and the result is a Hanle curve with a narrow dip ($\Delta B \sim 0.5$ mT), as shown in Fig. 24.

The magnitude of the apparent local field in the steady-state measurements can hence be ascribed to the field dependence of the nuclear spin relaxation time. This causes a decrease of the nuclear field at low values of the external magnetic field and hence an increased apparent local field.

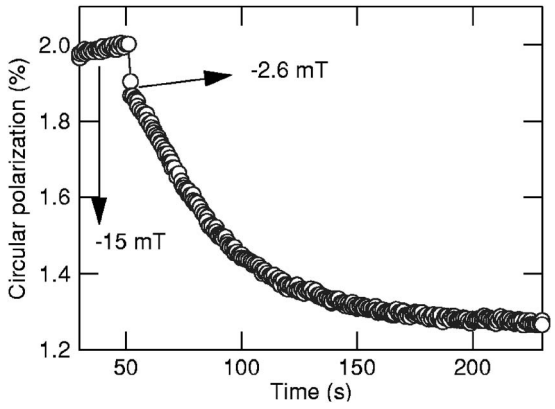

FIG. 23. Transient measurement to visualize the enhanced low-field nuclear relaxation at 5 K. The initial value of the external field is −15 mT, which is then rapidly swept to −2.6 mT. From this time the circular polarization of the electroluminescence starts to decrease to eventually reach its steady-state value.

D. Local field

The dip in Fig. 24 is asymmetric around zero field and the circular polarization becomes briefly negative during the field sweep. This last aspect can only be explained assuming an additional field in the semiconductor. First of all, as already discussed, the local field seen by the nuclei is given by the dipole field, the electronic field *and* the stray field from the ferromagnetic top layer. The dipole fields measured in earlier optical orientation measurements typically were measured in *p*-type layers codoped with silicon in order to achieve an efficient localization of the carriers. The localization assured that the nuclei were effectively polarized. In our case the nuclear spin relaxation time indicates that the dynamical nuclear polarization is caused by nuclear relaxation due to delocalized conduction band electrons. So unlike a mechanism of fast polarization by nuclei neighboring an impurity atom and a slower polarization of the bulk atoms by nuclear spin diffusion[17] the nuclei are homogeneously polarized by the conduction electrons. Hence they all experience the same electronic field. Increasing the carrier concentration can increase the value of this electronic field, that is given by[18]

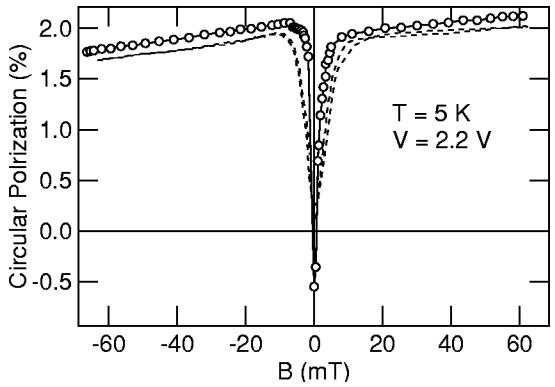

FIG. 24. The reconstructed Hanle curve at 5 K obtained using the method demonstrated in Fig. 23 (○) and the steady-state Hanle curve (dashed line).

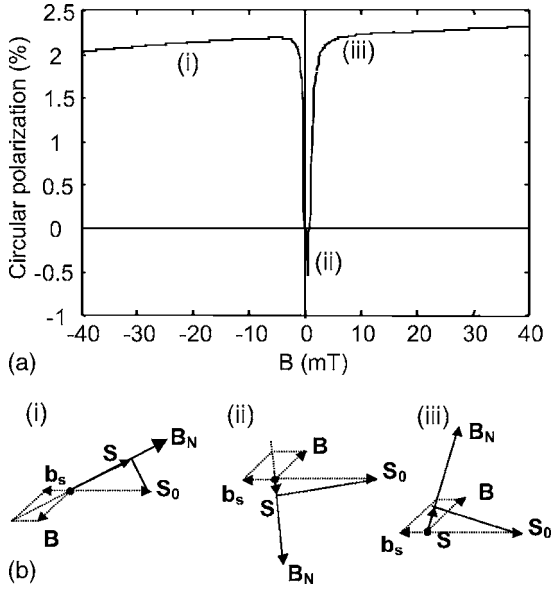

FIG. 25. (a) Simulation of the Hanle curve at 5 K, taking into account a stray field of 0.8 mT. (b) The different parts of the curve are schematically explained: (i) The average injected spin is in plane, pointing to the right. The stray field $\mathbf{b}_S$ induced by the MnSb film points to the left. The total field experienced by the nuclei is the sum of the external field $\mathbf{B}$ and the stray field $\mathbf{b}_S$ and is close to the external field. Hence, the direction of $\mathbf{B}_N$ is close to the direction of $\mathbf{B}$. The average electron spin $\mathbf{S}$ is the result of a projection of the injected electron spin $\mathbf{S}_0$ on the total field that acts on the electrons ($\sim\mathbf{B}_N$ when $\mathbf{B}_N$ is large). The observed circular polarization corresponds to the perpendicular component of the average electron spin and is positive in this case. (ii) At low (positive) values of $\mathbf{B}$, the total field that the nuclei experience and hence $\mathbf{B}_N$ points in the second quadrant. The perpendicular component of $\mathbf{S}$ then lies in the negative direction. (iii) $\mathbf{B}$ is again a lot stronger than the stray field and $\mathbf{B}$ lies again close to $\mathbf{B}$.

$$\Delta H = \tfrac{8}{3}\pi\langle|u_F(0)|^2\rangle\Omega_v \times \mu_B \times \Delta n, \tag{12}$$

with $\langle|u_F(0)|^2\rangle$ the squared Bloch function amplitude at the nucleus averaged on the Fermi surface, Ω_v the volume of the unit cell containing one Ga and one As atom, μ_B the Bohr magneton, and $\Delta n = n^{\uparrow} - n^{\downarrow}$, the difference between spin-up and spin-down electron concentrations. Taking $\langle|u_F(0)|^2\rangle = 5.8\times10^{25}$ cm^{-3} for the Ga atoms, $\langle|u_F(0)|^2\rangle = 9.8\times10^{25}$ cm^{-3} for the As atoms,[10] and $\Delta n = 4\times10^{16}$ cm^{-3} (using $n = 5\times10^{17}$ cm^{-3} and an electron spin polarization of 8%), the electronic field acting on the Ga nuclei is about 0.8 mT and the electronic field acting on the As nuclei is 1.35 mT. Still higher carrier concentrations only increase this electronic field. Due to the low polarization of the As nuclei, only the Ga value matters here.

Figure 25(a) shows a simulation using a local field of 0.5 mT and an additional stray field of 0.8 mT. It is schematically shown why this would lead to a negative circular polarization at low field: The nuclear spins always follow the total field acting on the nuclei and this field is the vector sum of the external field and the stray field. At an external field that is considerably larger than the stray field, the nuclear

spins always follow the external field. At low field however, the total field rotates toward the stray field. Since the average electron spin is the projection of the average injected spin on the total field acting on the electrons (=external field B +stray field b_S+nuclear field B_N), the circular polarization can become negative. The analysis taking into account the electronic field is similar and leads to a similar curve. The difference between the value of 0.8 mT and the predicted 0.2 mT can be caused by the simultaneous effect of the stray field and the electronic field. However, we cannot conclude from these measurements whether the additional local field mainly originates from the MnSb-induced stray field, the electronic field or a combination of both fields.

IV. CONCLUSIONS

We have investigated the pumping of nuclear spins due to electrical spin injection from a MnSb top contact through a Schottky tunnel barrier in a (Al,Ga)As spin LED using the oblique Hanle effect. Upon reversal of the MnSb magnetization (i.e., the injected electron spin polarization) or the external magnetic field, the measured degree of circular polarization exhibited slow transient effects that are correlated with slow changes in the nuclear spin system. The nuclear spin system has been shown to adiabatically reverse when reversing the external magnetic field. Nuclear magnetic resonance has shown that mainly the ^{71}Ga isotope is responsible for the observed effects. Especially the ^{75}As isotope is only weakly polarized, which we attribute to the more efficient quadrupolar spin relaxation of the As-nucleus.

Finally we have explained the enhanced width of the zero-field dip in the Hanle curve in our electrical pumping experiments as compared to optical pumping of compensated GaAs as the interplay between pumping and relaxation of the nuclear spins.

ACKNOWLEDGMENTS

We thank Willem van de Graaf and Stefan Degroote for MBE sample growth. We thank Vasyl Motsnyi and Wim Vanacken for experimental assistance and useful discussions. P.V.D. acknowledges financial support from the I.W.T. (Flanders) and W.V.R. from the F.W.O. (Belgium). This work was supported in part by the EC project SPINOSA (IST-2001-33334).

*Electronic address: pvandorp@imec.be

[1] *Optical Orientation*, edited by F. Meier and B. P. Zakharchenya (North-Holland, Amsterdam, 1984).
[2] J. Strand, B. D. Schultz, A. F. Isakovic, C. J. Palmström, and P. A. Crowell, Phys. Rev. Lett. **91**, 036602 (2003).
[3] A. T. Hanbicki, B. T. Jonker, G. Itskos, G. Kioseoglou, and A. Petrou, Appl. Phys. Lett. **80**, 1240 (2002).
[4] P. Van Dorpe, W. Van Roy, V. F. Motsnyi, G. Borghs, and J. De Boeck, J. Vac. Sci. Technol. A **22**, 1862 (2004).
[5] W. Van Roy, P. Van Dorpe, V. F. Motsnyi, Z. Liu, G. Borghs, and J. De Boeck, Phys. Status Solidi B **241**(7), 1470 (2004).
[6] The simulations were performed using Medici, a commercial semiconductor simulation tool that allows self-consistent simulations including, e.g., Schottky barrier tunneling.
[7] H. Akinaga, S. Miyanishi, W. Van Roy, J. De Boeck, and G. Borghs, Appl. Phys. Lett. **73**, 3285 (1998).
[8] V. F. Motsnyi, V. I. Safarov, J. De Boeck, J. Das, W. Van Roy, E. Goovaerts, and G. Borghs, Appl. Phys. Lett. **81**, 265 (2002).
[9] V. F. Motsnyi, P. Van Dorpe, W. Van Roy, E. Goovaerts, V. I. Safarov, G. Borghs, and J. De Boeck, Phys. Rev. B **68**, 245319 (2003).
[10] M. I. D'Yakonov and V. I. Perel, Sov. Phys. JETP **38** (1), 177 (1974).
[11] A. Abragam, *Principles of Nuclear Magnetism* (Oxford University Press, Oxford, 1961).
[12] J. Strand, A. F. Isakovic, X. Lou, P. A. Crowell, B. D. Schultz, and C. J. Palmström, Appl. Phys. Lett. **83**, 3335 (2003).
[13] L. C. Hebel and C. P. Slichter, Phys. Rev. **113**, 1504 (1959).
[14] D. Paget, G. Lampel, B. Sapoval, and V. I. Safarov, Phys. Rev. B **15**, 5780 (1977).
[15] R. L. Mieher, Phys. Rev. **125** (5), 1537 (1962).
[16] R. K. Kawakami, Y. Kato, M. Hanson, I. Malajovich, J. M. Stephens, E. Johnston-Halperin, G. Salis, A. C. Gossard, and D. D. Awschalom, Science **294**, 131 (2001).
[17] D. Paget, Phys. Rev. B **25**, 4444 (1982).
[18] G. A. Miranda, J. A. McNeil, and W. G. Clark, Phys. Rev. B **9**, 495 (1974).